Drosophila Microbiome Modulates Host Developmental and Metabolic Homeostasis via Insulin Signaling

Seung Chul Shin *et al.*

Science **334**, 670 (2011);
DOI: 10.1126/science.1212782

Science (print ISSN 0036-8075; online ISSN 1095-9203) is published weekly, except the last week in December, by the American Association for the Advancement of Science, 1200 New York Avenue NW, Washington, DC 20005.

information from the leader may be preferentially represented in the brains of both individuals. Finally, coordination of timing during cooperation is likely mediated by interactions between CPGs and both autogenous and heterogenous sensory information.

References and Notes

1. R. Noë, *Anim. Behav.* **71**, 1 (2006).
2. M. P. Crawford, *Comp. Psychol. Monogr.* **14**, 1 (1937).
3. N. S. Clayton, J. M. Dally, N. J. Emery, *Philos. Trans. R. Soc. London B Biol. Sci.* **362**, 507 (2007).
4. F. Péron, L. Rat-Fischer, M. Lalot, L. Nagle, D. Bovet, *Anim. Cogn.* **14**, 545 (2011).
5. D. J. Wheatcroft, T. D. Price, *Trends Ecol. Evol.* **23**, 416 (2008).
6. D. J. Hoare, I. D. Couzin, J. G. J. Godin, J. Krause, *Anim. Behav.* **67**, 155 (2004).
7. N. I. Mann, F. K. Barker, J. A. Graves, K. A. Dingess-Mann, P. J. Slater, *Mol. Phylogenet. Evol.* **40**, 750 (2006).
8. N. I. Mann, K. A. Dingess, K. F. Barker, J. A. Graves, P. J. Slater, *Behaviour* **146**, 1 (2009).
9. N. I. Mann, K. A. Dingess, P. J. Slater, *Biol. Lett.* **2**, 1 (2006).
10. M. A. Long, D. Z. Jin, M. S. Fee, *Nature* **468**, 394 (2010).
11. E. T. Vu, M. E. Mazurek, Y. C. Kuo, *J. Neurosci.* **14**, 6924 (1994).
12. M. A. Long, M. S. Fee, *Nature* **456**, 189 (2008).
13. D. Margoliash *et al.*, *Brain Behav. Evol.* **44**, 247 (1994).
14. N. Tinbergen, *The Study of Instinct* (Oxford Univ. Press, New York, 1951).
15. D. M. Logue, C. Chalmers, H. A. Gowland, *Anim. Behav.* **75**, 1803 (2008).
16. D. M. Logue, *Anim. Behav.* **73**, 105 (2007).
17. R. N. Levin, *Anim. Behav.* **52**, 1107 (1996).
18. E. S. Fortune, D. Margoliash, *J. Comp. Neurol.* **360**, 413 (1995).
19. F. Nottebohm, T. M. Stokes, C. M. Leonard, *J. Comp. Neurol.* **165**, 457 (1976).
20. R. Mooney, *J. Neurosci.* **20**, 5420 (2000).
21. D. Margoliash, *J. Neurosci.* **6**, 1643 (1986).
22. D. Margoliash, *J. Neurosci.* **3**, 1039 (1983).
23. R. Mooney, W. Hoese, S. Nowicki, *Proc. Natl. Acad. Sci. U.S.A.* **98**, 12778 (2001).
24. T. A. Nick, M. Konishi, *J. Neurobiol.* **62**, 469 (2005).
25. M. J. Coleman, R. Mooney, *J. Neurosci.* **24**, 7251 (2004).
26. M. M. Solis, A. J. Doupe, *J. Neurosci.* **17**, 6447 (1997).
27. J. F. Prather, S. Peters, S. Nowicki, R. Mooney, *Nature* **451**, 305 (2008).
28. A. S. Dave, D. Margoliash, *Science* **290**, 812 (2000).
29. D. Margoliash, E. S. Fortune, *J. Neurosci.* **12**, 4309 (1992).
30. C. J. Edwards, T. B. Alder, G. J. Rose, *Nat. Neurosci.* **5**, 934 (2002).

Acknowledgments: This research would not have been possible without the help and support of S. Burneo, curator, Museum of Zoology (QCAZ), Pontificia Universidad Católica del Ecuador in Quito. This project used equipment previously purchased with funds from NSF award IOS-0817918 to E.S.F. Support was also provided by the Johns Hopkins University and Claremont McKenna, Pitzer, Scripps Colleges. We thank H. Greeney, J. Simbaña, R. Jarrín, A. Saa, and K. Cisneros for logistical support; N. Cowan, J. Knierim, R. Krahe, and H. Zakon for helpful discussions and feedback; and D. Margoliash for his advice and insights. Behavioral and neurophysiological data are available upon request. Animal tissues are archived in the QCAZ in Quito, Ecuador, and are available in accordance with the relevant laws and regulations of the Republic of Ecuador.

Supporting Online Material

www.sciencemag.org/cgi/content/full/334/6056/666/DC1
Materials and Methods
Fig. S1
References
Audio Clips S1 to S5
Movies S1 and S2

15 June 2011; accepted 6 September 2011
10.1126/science.1209867

Drosophila Microbiome Modulates Host Developmental and Metabolic Homeostasis via Insulin Signaling

Seung Chul Shin,[1,3]*† Sung-Hee Kim,[1]† Hyejin You,[1,2] Boram Kim,[1,2] Aeri C. Kim,[1,2] Kyung-Ah Lee,[1] Joo-Heon Yoon,[3] Ji-Hwan Ryu,[3] Won-Jae Lee[1]‡

The symbiotic microbiota profoundly affect many aspects of host physiology; however, the molecular mechanisms underlying host-microbe cross-talk are largely unknown. Here, we show that the pyrroloquinoline quinone–dependent alcohol dehydrogenase (PQQ-ADH) activity of a commensal bacterium, *Acetobacter pomorum*, modulates insulin/insulin-like growth factor signaling (IIS) in *Drosophila* to regulate host homeostatic programs controlling developmental rate, body size, energy metabolism, and intestinal stem cell activity. Germ-free animals monoassociated with *PQQ-ADH* mutant bacteria displayed severe deregulation of developmental and metabolic homeostasis. Importantly, these defects were reversed by enhancing host IIS or by supplementing the diet with acetic acid, the metabolic product of PQQ-ADH.

All metazoans harbor substantial numbers of commensal microorganisms in the gut. It has been well established that commensal bacteria have positive impacts across a wide range of host physiology, including regulation of immunity and metabolism (*1*–*3*). Recent progress toward understanding gut-microbe interactions using *Drosophila* revealed that a fine-tuned regulation of gut immunity is required for the preservation of a healthy commensal community structure to promote host fitness and ensure normal host survival rates (*4*). Furthermore, the indigenous gut microbiota also controls the normal turnover rate of gut epithelial cells by regulating intestinal stem cell activity (*5*).

Recently, it has been shown that the normal microflora is deeply involved in the energy balance and metabolic homeostasis of host animals (*6*–*9*). However, our current understanding of the impact of gut microbiota on host physiology is descriptive, due in part to technical difficulties associated with in-depth integrated genetic analysis of both the microbes and the host. To overcome these limitations, we used the combination of *Drosophila* and its commensal *Acetobacter* as a model of host-microbe interaction to enable us to perform a simultaneous genetic analysis of both host and microbe in vivo.

To observe the systemic effects of the symbiotic commensal community on the host, we first examined host growth rate and body size in the presence and absence of the commensal microflora by generating conventionally reared and germ-free animals (*10*). In conventionally reared fly larvae, the time to develop into a puparium was <7 days; it lengthened to ~9 days in germ-free larvae when they fed on the axenic standard cornmeal diet (Fig. 1A). Interestingly, the effect of commensal bacteria on host development was more pronounced when the amount of yeast in the diet was reduced (Fig. 1A and fig. S1). Most notably, conventionally reared larvae developed into puparia in ~9 days, whereas germ-free larvae died at first instar if fed a diet containing <0.1% yeast or if yeast was substituted by casamino acids (Fig. 1A and fig. S1). Casamino acids were found to be essential nutrients for host growth in the absence of yeast. Under these conditions, germ-free larvae had a body size <10% of corresponding conventionally reared larvae 120 hours after egg laying (Fig. 1A and fig. S1). At this time point, the effect of the microbiota on host growth was most pronounced. These results indicate that commensal microbiota is able to influence the systemic development of *Drosophila* by affecting both growth rate and body size.

All metazoan guts harbor complex commensal communities: hundreds of species are present in humans (*11*). In *Drosophila*, the adult midgut is typically in stable contact with a symbiotic commensal community composed of 5 to 20 different microbial species that consist primarily of members of the *Acetobacter* and *Lactobacillus* genera (*12*–*14*). We found that the midgut of laboratory-reared *Drosophila* harbors five major commensal bacterial species, *Commensalibacter intestini*, *Acetobacter pomorum*, *Gluconobacter morbifer*, *Lactobacillus plantarum*, and *Lactobacillus brevis* (*12*, *15*). Taking advantage of

[1]School of Biological Science, Seoul National University and National Creative Research Initiative Center for Symbiosystem, Seoul 151-742, South Korea. [2]Department of Bioinspired Science and Division of Life and Pharmaceutical Science, Ewha Woman's University, Seoul 120-750, South Korea. [3]Research Center for Human Natural Defense System, Yonsei University College of Medicine, CPO Box 8044 Seoul, South Korea.

*Present address: Korea Polar Research Institute, Incheon 406-840, South Korea.

†These authors contributed equally to this work.

‡To whom correspondence should be addressed. E-mail: lwj@snu.ac.kr

this simple commensal community, we examined whether the beneficial role of commensal microbiota is attributed to the combined effects of whole commensal community or whether it can be attributed to the activities of a subset of the microbiota. We exposed germ-free embryos fed on medium containing casamino acids instead of yeast to each of the five species of commensal bacteria and found that all were able to colonize the host gut independently. Colonization of *A. pomorum* alone in the germ-free gut was sufficient for restoring the developmental rate and body size of casamino acid–fed larvae such that the developmental rate and body size of the host animals were comparable to those of conventionally reared larvae or germ-free larvae colonized by all five bacteria species (Fig. 1B). The other four bacteria species had a minor effect on larval growth and development (Fig. 1B).

Acetic acid bacteria such as *Asaia* sp. colonize gut epithelial cells of mosquito (*Anopheles* sp.) through a specific association between the insect epithelial cells and extracellular polysaccharide matrix that surrounds bacterial cells (*16*, *17*). Because our *A. pomorum* strain also produced large quantities of extracellular polysaccharides (when cultured in vitro, we observed a thick layer of extracellular polysaccharides), contact between *Drosophila* gut epithelial cells and *A. pomorum* may be similar to that observed between *Asaia* and *Anopheles* gut cells. To understand the beneficial role of *A. pomorum* on host developmental homeostasis at the molecular level, we established a draft genome sequence of *A. pomorum* with a whole-genome shotgun strategy and subsequently performed a transposon Tn5-mediated random mutagenesis to generate an *A. pomorum* mutant library. The draft genome sequence of *A. pomorum* consisting of 67 contigs in 19 scaffolds contains 2696 predicted genes with a total genome size of ~2.8 Mb. To screen for bacterial genes conferring benefits on the host, we measured growth rate and body size for each cohort of fly larvae colonized by each mutant ($N \sim 3000$ each) 120 hours after egg laying (fig. S2). We performed two replicates of the genome-wide screening.

We found that 23 cohorts of mutant *A. pomorum*–monoassociated larvae were consistently smaller compared with the wild-type (WT) *A. pomorum*–monoassociated larvae. Analysis of the molecular lesions in the 23 mutant strains identified 14 genes, including 11 genes involved in the periplasmic pyrroloquinoline quinone–dependent alcohol dehydrogenase (PQQ-ADH)–dependent oxidative respiratory chain and three genes encoding proteins with other functions (figs. S3 and S4 and table S1). Larvae colonized with any of the 14 mutant strains showed developmental defects (Fig. 1C), although the bacteria colonized the larval gut as efficiently as WT *A. pomorum* (fig. S5).

Given that the majority of the bacterial genes we identified as having a growth-promoting effect on their host are known to be involved in the PQQ-ADH–dependent oxidative respiratory chain (fig. S3) and that five different mutations in the *PQQ-ADH-I* gene were independently identified (fig. S4 and table S1), we focused on the role of bacterial *PQQ-ADH-I* on host physiology. Among the five mutants, we subsequently used *P3G5* for in-depth analyses. The *P3G5* strain itself exhibited a similar in vitro growth rate to that of the parental WT *A. pomorum* and colonized gut epithelia as efficiently as WT *A. pomorum* (fig. S6). Under this condition, we observed that the development time to reach puparium formation extended to ~14 days in *P3G5*-monoassociated larvae compared with <10 days in WT *A. pomorum*–monoassociated larvae (Fig. 2A). In low yeast medium, we observed similar results to those from larvae fed on casamino acids (Fig. 2A). Control experiments showed that the feeding rate between WT *A. pomorum*– and *P3G5*-monoassociated larvae did not differ (fig. S7). In addition to a slower larval developmental rate, we found that *P3G5*-monoassociated adults were significantly

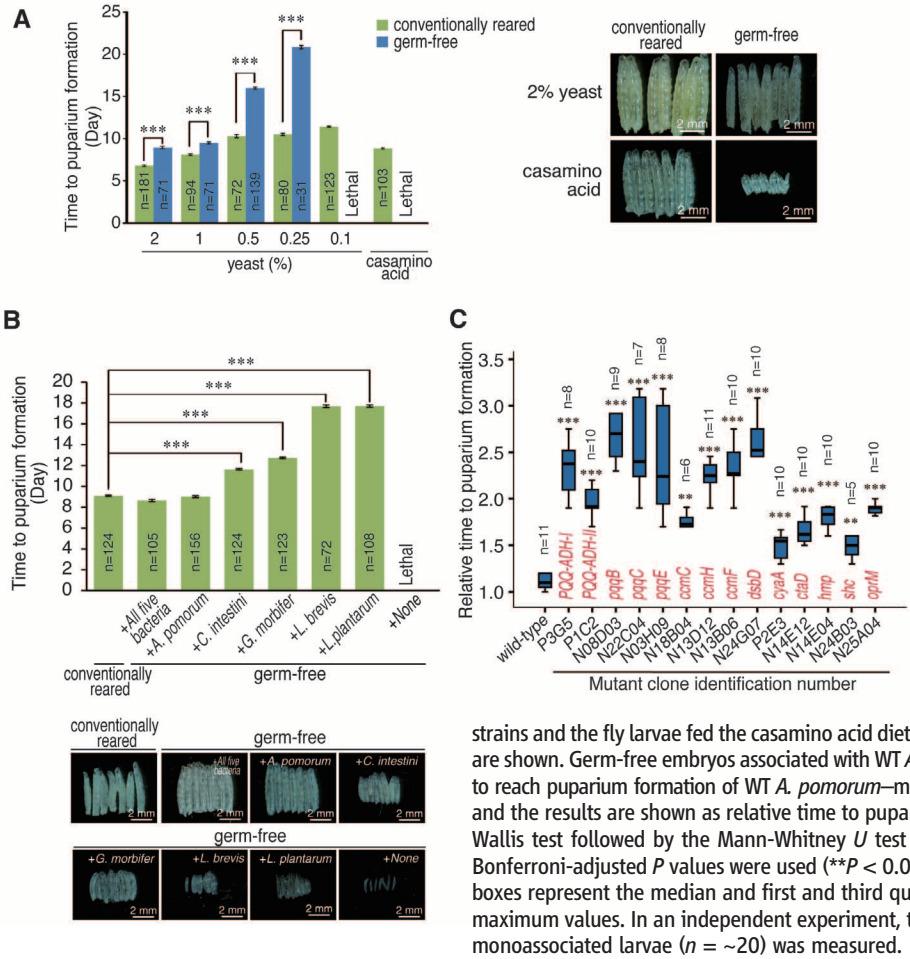

Fig. 1. Genome-wide screening of the *Acetobacter* genes essential for host growth. (**A**) The time to reach puparium formation of conventionally reared w^{1118} larvae and germ-free w^{1118} larvae fed a standard laboratory diet containing different yeast concentrations (2, 1, 0.5, 0.25, or 0.1%) or the casamino acid diet (casamino acid). The sizes of larvae at the 120th hour of development after egg laying are shown. Data were analyzed using an analysis of variance (ANOVA) followed by Tamhane's T2 post hoc test; values represent mean ± SEM (***$P < 0.001$). (**B**) *A. pomorum* is sufficient for full larval development. Germ-free embryos were associated with each of the five species of commensal bacteria or all five commensal bacteria (+*A. pomorum*/*C. intestini*/*G. morbifer*/*L. plantarum*/*L. brevis*). Germ-free embryos and conventionally reared embryos were also used as control. The time to reach puparium formation was measured in the casamino acid diet. The sizes of larvae at the 120th hour of development after egg laying are shown. Data were analyzed using an ANOVA followed by Tamhane's T2 post hoc test; values represent mean ± SEM (***$P < 0.001$). (**C**) All 14 screened mutant strains were defective in promoting host development. Germ-free embryos were colonized with each of the 14 mutant *A. pomorum* strains and the fly larvae fed the casamino acid diet. Mutated gene names and clone identification numbers are shown. Germ-free embryos associated with WT *A. pomorum* (wild-type) were used as the control. The time to reach puparium formation of WT *A. pomorum*–monoassociated embryos was arbitrarily designated as 1, and the results are shown as relative time to puparium formation. Data were analyzed using the Kruskal-Wallis test followed by the Mann-Whitney *U* test using Bonferroni correction to adjust the probability. Bonferroni-adjusted *P* values were used (**$P < 0.01$, ***$P < 0.001$). In box-plot diagrams, black lines and boxes represent the median and first and third quartiles of the values; whiskers extend to minimum and maximum values. In an independent experiment, the time to reach puparium formation of each group of monoassociated larvae (n = ~20) was measured.

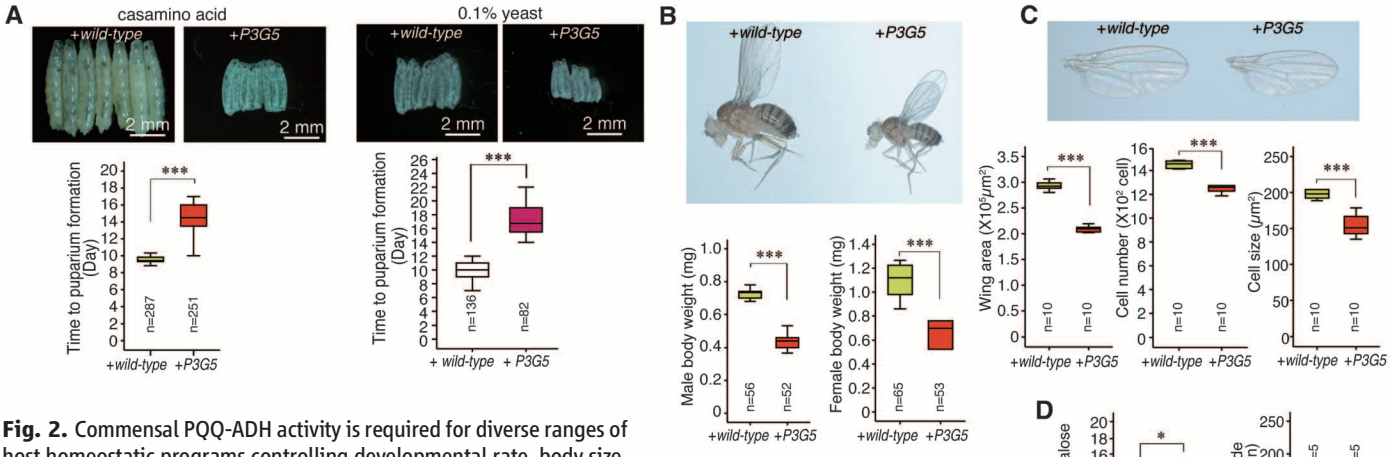

Fig. 2. Commensal PQQ-ADH activity is required for diverse ranges of host homeostatic programs controlling developmental rate, body size, and metabolism. In all experiments, germ-free embryos monoassociated with the WT *A. pomorum* (*+wild-type*) and *P3G5* mutant strain (*+P3G5*) maintained in the casamino acid media were compared. (**A**) Time to puparium formation and sizes of larvae 120 hours after egg laying. A standard cornmeal-agar medium containing 0.1% yeast was also used. Data were analyzed using the Mann-Whitney *U* test (***$P < 0.001$). (**B**) Adult body sizes. Body weights of adult flies (5 days old) were measured. Data were analyzed using the Mann-Whitney *U* test (***$P < 0.001$). (**C**) Wing area, cell number, and size. Female adult flies (5 days old) were used. Data were analyzed using the Mann-Whitney *U* test (***$P < 0.001$). (**D**) Sugar and lipid levels. The early third instar larvae (10 to 15 larvae per each experiment) were used. Data were analyzed using the Mann-Whitney *U* test (*$P < 0.05$ and **$P < 0.01$).

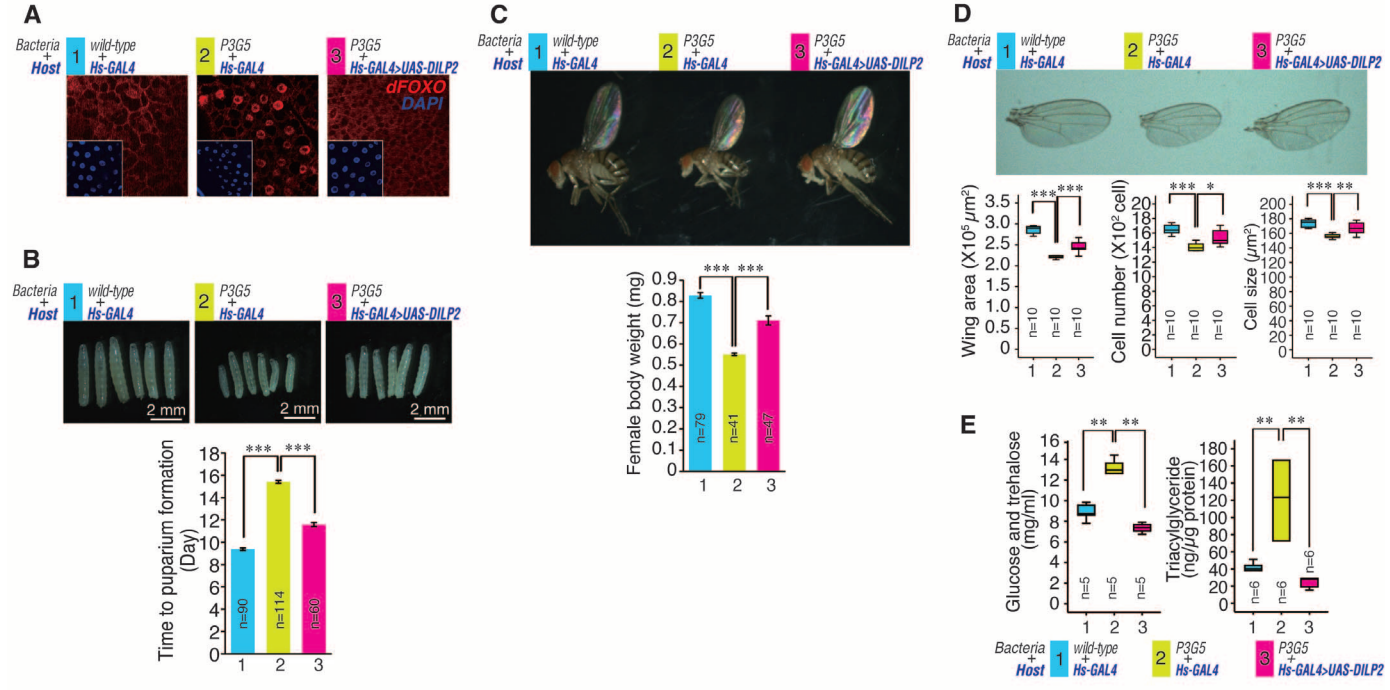

Fig. 3. Deregulation of developmental and metabolic homeostasis in *P3G5*-monoassociated animals is rescued by enhancing host IIS. In all experiments, animals maintained in the casamino acid media were compared. The animals used in this study were: *wild-type* + *Hs-GAL4*, WT *A. pomorum*-monoassociated control flies carrying *Hs-GAL4* alone; *P3G5* + *Hs-GAL4*, *P3G5*-monoassociated control flies carrying *Hs-GAL4* alone; and *P3G5* + *Hs-GAL4>UAS-DILP2*, *P3G5*-monoassociated flies carrying *Hs-GAL4>UAS-DILP2*. (**A**) *P3G5*-induced dFOXO nuclear localization is abolished upon ectopic *DILP2* expression leading to cytoplasmic retention of dFOXO. Fat body tissues of the early third instar larvae were used. (**B**) Time to puparium formation and the sizes of the larvae at the 120th hour of development after egg laying. Data are analyzed using an ANOVA followed by Tamhane's T2 post hoc test; values represent mean ± SEM (***$P < 0.001$). (**C**) Adult body size. Body weights of female adults (5 days old) were measured. Data are analyzed using an ANOVA followed by Tamhane's T2 post hoc test; values represent mean ± SEM (***$P < 0.001$). (**D**) Wing area, cell number, and size. Wings of female adult flies (5 days old) were used in this study. Data were analyzed using Kruskal-Wallis test followed by the Mann-Whitney *U* test using Bonferroni correction to adjust the probability. Bonferroni-adjusted *P* values were used (*$P < 0.05$, **$P < 0.01$, ***$P < 0.001$). (**E**) Sugar and lipid levels. The early third instar larvae (10 to 15 larvae per each experiment) were used. Data were analyzed using Kruskal-Wallis test followed by the Mann-Whitney *U* test using Bonferroni correction to adjust the probability. Bonferroni-adjusted *P* values were used (**$P < 0.01$).

smaller than WT *A. pomorum*–monoassociated adults (Fig. 2B). Consistent with smaller body size, *P3G5*-monoassociated adults had smaller wings, with reduced cell size and number, compared with those of control adults (Fig. 2C), and also small intestines (fig. S7). Furthermore, we found that PQQ-ADH activity of *A. pomorum* ensured the basal number of intestine stem cells (ISCs) and the epithelial cell renewal rate via induction of *Unpaired-3* (*Upd3*) expression for Janus kinase–signal transducers and activators of transcription signaling activation (fig. S8).

The overall body and tissue size reduction observed in the *P3G5*-monoassociated animals is reminiscent of animals with defective insulin/insulin-like growth factor signaling (IIS) (*18*–*22*). It is known that IIS mutant animals show diabetic phenotypes, including an increase in circulating sugars and stored lipid levels (*20*, *23*, *24*). When we examined the levels of sugars and lipids in *P3G5*-monoassociated larvae, we found elevated levels of total sugars [glucose and trehalose (the major disaccharide in insects)] and triacylglycerides (the main form of stored lipids) compared with those seen in control larvae (Fig. 2D). Consistent with the IIS mutant-like phenotype, we found that WT *A. pomorum*, but not *P3G5*, was able to induce IIS activation as evidenced by phosphoinositide 3-kinase (PI3K) activation and cytoplasmic retention of the forkhead transcription factor (dFOXO) (fig. S9). Furthermore, bacterial PQQ-ADH activity is required for full expression of *Drosophila* insulin-like peptides (*DILPs*) in the larval brain, suggesting that PQQ-ADH activity contributes to IIS activation in part through *DILP* induction (fig. S9). Importantly, we did not observe all the effects of WT *A. pomorum* on host developmental and metabolic homeostasis in the absence of host IIS activation (fig. S10), indicating that *A. pomorum* affects host physiological homeostasis through IIS activation.

To further investigate whether metabolic and developmental defects found in a *P3G5*-monoassociated animal were caused by low IIS pathway activity, we attempted to restore host homeostasis by enhancing IIS activity through ectopic overexpression of *DILP2* (*Hs-GAL4>UAS-DILP2*) in *P3G5*-monoassociated animals. The results (Fig. 3A) show that dFOXO nuclear localization in the fat body, seen in the *P3G5*-monoassociated control larvae (carrying the *Hs-GAL4* driver alone), was abolished upon ectopic *DILP2* expression (that is, *P3G5*-monoassociated *Hs-GAL4>UAS-DILP2* larvae), leading to cytoplasmic retention of dFOXO. Importantly, all metabolic and developmental defects (Fig. 3, B to E), as well as ISC deregulation (fig. S11) caused by *P3G5* bacteria were largely rescued in *P3G5*-monoassociated *Hs-GAL4>UAS-DILP2* animals. Interestingly, *DILP* overexpression could not rescue developmental defects found in germ-free larvae monoassociated with other non–*A. pomorum* commensal bacteria (fig. S12), indicating that the *DILP* effect is specific for *P3G5*-monoassociated animals.

PQQ-ADH is the primary dehydrogenase in the ethanol oxidative respiratory chain of *Acetobacter* involved in acetic acid production (*25*). We found that all screened mutant bacteria including the *P3G5* strain showed impaired or severely reduced acetic acid production (fig. S13),

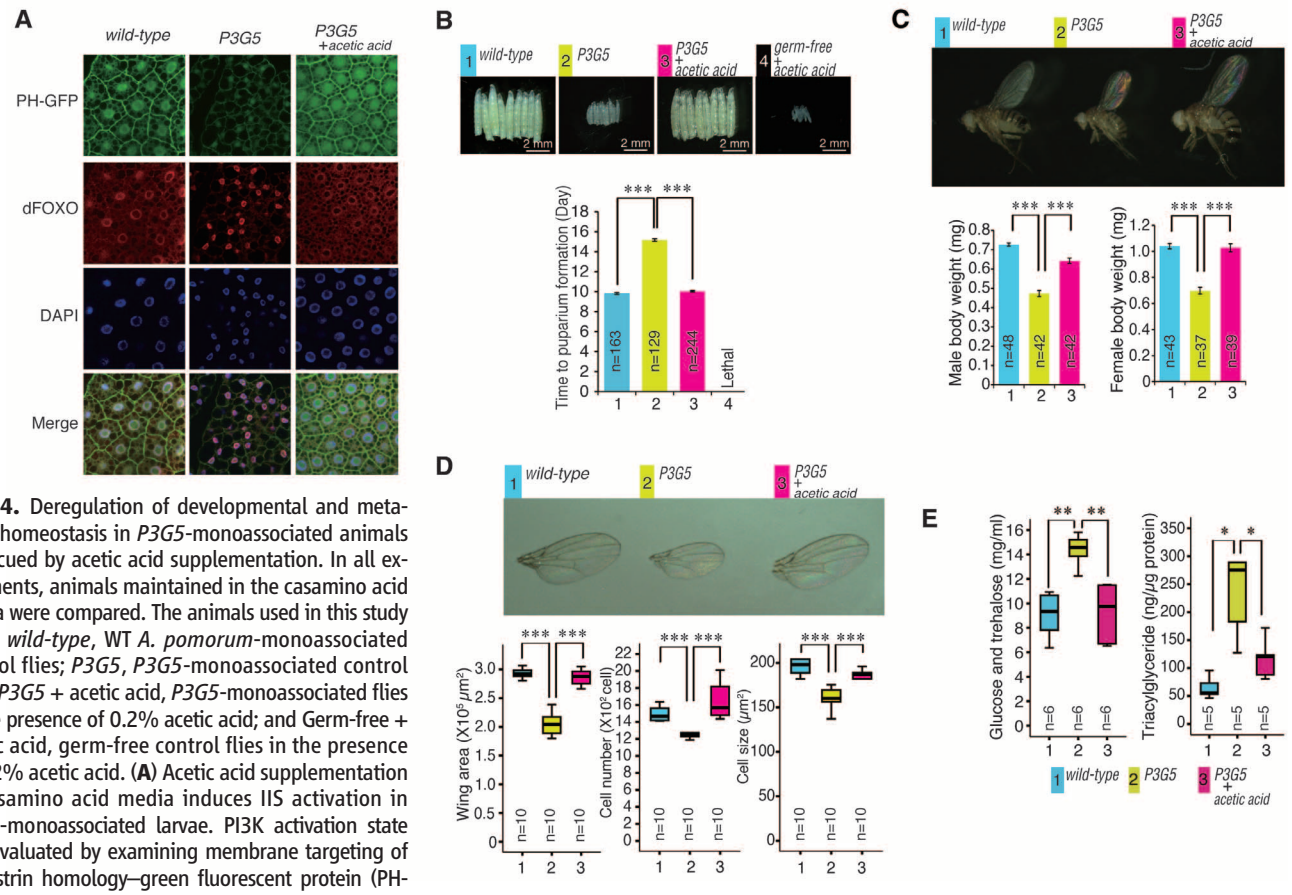

Fig. 4. Deregulation of developmental and metabolic homeostasis in *P3G5*-monoassociated animals is rescued by acetic acid supplementation. In all experiments, animals maintained in the casamino acid media were compared. The animals used in this study were: *wild-type*, WT *A. pomorum*-monoassociated control flies; *P3G5*, *P3G5*-monoassociated control flies; *P3G5* + acetic acid, *P3G5*-monoassociated flies in the presence of 0.2% acetic acid; and Germ-free + acetic acid, germ-free control flies in the presence of 0.2% acetic acid. (**A**) Acetic acid supplementation in casamino acid media induces IIS activation in *P3G5*-monoassociated larvae. PI3K activation state was evaluated by examining membrane targeting of pleckstrin homology–green fluorescent protein (PH-GFP), and localization of dFOXO was examined by immunostaining with an antibody to dFOXO. Fat body tissues of the early third instar larvae were used. DAPI, 4′,6-diamidino-2-phenylindole. (**B**) Time to puparium formation, and sizes of larvae at the 120th hour of development after egg laying. Data were analyzed using an ANOVA followed by Tamhane's T2 post hoc test. Values represent mean ± SEM (***$P < 0.001$). (**C**) Adult body size. Body weights of adult flies (5 days old) were measured. Data were analyzed using an ANOVA followed by Tamhane's T2 post hoc test; values represent mean ± SEM (***$P < 0.001$). (**D**) Wing area, cell number, and size. Wings of female adult flies (5 days old) were used in this study. Data were analyzed using the Kruskal-Wallis test followed by the Mann-Whitney *U* test using Bonferroni correction to adjust the probability. Bonferroni-adjusted *P* values were used (***$P < 0.001$). (**E**) Sugar and lipid levels. The early third instar larvae (10 to 15 larvae per each experiment) were used. Data were analyzed using the Kruskal-Wallis test followed by the Mann-Whitney *U* test using Bonferroni correction to adjust the probability. Bonferroni-adjusted *P* values were used (*$P < 0.05$, **$P < 0.01$).

suggesting that acetic acid–producing ability is an important factor that affects host physiology. Although acetic acid supplementation in casamino acid media did not result in any appreciable effect on host development in the absence of bacteria (i.e., germ-free animals) or in the presence of commensal bacterium other than *A. pomorum* (i.e., germ-free animals monoassociated with *C. intestini*, *G. morbifer*, *L. plantarum*, or *L. brevis*), all disease phenotypes (defects in IIS, development, metabolism and ISCs) found in *P3G5*-monoassociated animals could be effectively reversed by acetic acid supplementation (Fig. 4 and fig. S13). Although the exact mechanism of acetic acid action remains to be elucidated, it is known to affect blood glucose level and insulin signaling in mammals by reducing the digestion rate of complex carbohydrates in the diet (*26*). However, the aforementioned *P3G5*-induced deregulation found when the fly larvae were fed a complex carbohydrate diet (i.e., containing cornmeal) was also observed in fly larvae fed a diet containing simple carbohydrates, such as sucrose or glucose (fig. S13). Furthermore, these defects were reversed by supplementing the simple sugar diet with acetic acid (fig. S13), indicating that acetic acid may influence host IIS and development through a mechanism other than by reducing the digestion rate of complex carbohydrates from the diet. Given that acetic acid can rescue host physiology only in the presence of *P3G5* bacterial metabolic activity, we can conclude that both PQQ-ADH–dependent acetic acid generation and PQQ-ADH–independent acetic acid metabolism are required to promote the effect of *A. pomorum* on host IIS. Further dissection of the *A. pomorum*–controlled gut factor(s) that mediates the effect of acetic acid–producing and –using bacterial metabolic activity on host IIS will provide an important link between gut microbiome activity and host metabolic homeostasis.

In summary, the present study showed that the PQQ-ADH respiratory chain of the *A. pomorum* and IIS of the host interact to maintain the gut-microbe mutualism. Bacterial PQQ-ADH is required, but not sufficient, to explain all of the *A. pomorum*–mediated effects on host physiology, and host signaling pathways, other than IIS, may also be modulated by gut bacteria. Our *Drosophila-Acetobacter* interaction system is a useful genetic model for understanding the mechanistic links between microbiome-modulated host signaling pathways and host physiology.

References and Notes

1. F. Bäckhed, R. E. Ley, J. L. Sonnenburg, D. A. Peterson, J. I. Gordon, *Science* **307**, 1915 (2005).
2. T. A. Koropatnick *et al.*, *Science* **306**, 1186 (2004).
3. J. L. Round *et al.*, *Science* **332**, 974 (2011); 10.1126/science.1206095.
4. Y. S. Bae, M. K. Choi, W. J. Lee, *Trends Immunol.* **31**, 278 (2010).
5. N. Buchon, N. A. Broderick, S. Chakrabarti, B. Lemaitre, *Genes Dev.* **23**, 2333 (2009).
6. M. Vijay-Kumar *et al.*, *Science* **328**, 228 (2010); 10.1126/science.1179721.
7. P. J. Turnbaugh *et al.*, *Nature* **444**, 1027 (2006).
8. A. M. O'Hara, F. Shanahan, *EMBO Rep.* **7**, 688 (2006).
9. P. J. Turnbaugh *et al.*, *Nature* **457**, 480 (2009).
10. Materials and methods are available as supporting material on *Science* Online.
11. J. Qin *et al.*; MetaHIT Consortium, *Nature* **464**, 59 (2010).
12. J.-H. Ryu *et al.*, *Science* **319**, 777 (2008); 10.1126/science.1149357.
13. C. Ren, P. Webster, S. E. Finkel, J. Tower, *Cell Metab.* **6**, 144 (2007).
14. C. N. Wong, P. Ng, A. E. Douglas, *Environ. Microbiol.* **13**, 1889 (2011).
15. S. W. Roh *et al.*, *Appl. Environ. Microbiol.* **74**, 6171 (2008).
16. E. Crotti *et al.*, *Environ. Microbiol.* **11**, 3252 (2009).
17. G. Favia *et al.*, *Proc. Natl. Acad. Sci. U.S.A.* **104**, 9047 (2007).
18. B. A. Edgar, *Nat. Rev. Genet.* **7**, 907 (2006).
19. W. Brogiolo *et al.*, *Curr. Biol.* **11**, 213 (2001).
20. E. J. Rulifson, S. K. Kim, R. Nusse, *Science* **296**, 1118 (2002).
21. M. Tatar *et al.*, *Science* **292**, 107 (2001).
22. K. D. Baker, C. S. Thummel, *Cell Metab.* **6**, 257 (2007).
23. R. Böhni *et al.*, *Cell* **97**, 865 (1999).
24. S. J. Broughton *et al.*, *Proc. Natl. Acad. Sci. U.S.A.* **102**, 3105 (2005).
25. T. Yakushi, K. Matsushita, *Appl. Microbiol. Biotechnol.* **86**, 1257 (2010).
26. C. S. Johnston, I. Steplewska, C. A. Long, L. N. Harris, R. H. Ryals, *Ann. Nutr. Metab.* **56**, 74 (2010).

Acknowledgments: This work was supported by the National Creative Research Initiative Program (to W.-J.L.), the BK 21 program, the Basic Science Research Program (2011-0001168, to J.-H.R. and J.-H.Y.), and a Gwangju Institute of Science and Technology–Systems Biology grant (2011) of the Ministry of Science and Technology Korea. We thank D. Daffonchio and K. Matsushita for helpful comments on *Acetobacter*. The *A. pomorum* draft genome sequence is deposited in DNA Data Bank of Japan/European Molecular Biology Laboratory/GenBank with accession no. AEUP01000000.

Supporting Online Material

www.sciencemag.org/cgi/content/full/334/6056/670/DC1
Materials and Methods
Figs. S1 to S13
Table S1
References (*27*–*37*)

16 August 2011; accepted 8 September 2011
10.1126/science.1212782

N-Terminal Acetylation Acts as an Avidity Enhancer Within an Interconnected Multiprotein Complex

Daniel C. Scott,[1,2] Julie K. Monda,[1] Eric J. Bennett,[3]* J. Wade Harper,[3] Brenda A. Schulman[1,2]†

Although many eukaryotic proteins are amino (N)–terminally acetylated, structural mechanisms by which N-terminal acetylation mediates protein interactions are largely unknown. Here, we found that N-terminal acetylation of the E2 enzyme, Ubc12, dictates distinctive E3-dependent ligation of the ubiquitin-like protein Nedd8 to Cul1. Structural, biochemical, biophysical, and genetic analyses revealed how complete burial of Ubc12's N-acetyl-methionine in a hydrophobic pocket in the E3, Dcn1, promotes cullin neddylation. The results suggest that the N-terminal acetyl both directs Ubc12's interactions with Dcn1 and prevents repulsion of a charged N terminus. Our data provide a link between acetylation and ubiquitin-like protein conjugation and define a mechanism for N-terminal acetylation-dependent recognition.

Many eukaryotic proteins are N-terminally acetylated (*1*–*4*). Genetic data underscore the importance of N-terminal methionine acetylation (*1*, *5*–*10*), although specific interactions mediated by N-acetyl-methionine are largely unknown. We examined how N-acetyl-methionine can direct protein interactions by studying an E2 enzyme. E2s play central roles in E1→E2→E3 ubiquitin-like protein (UBL) conjugation cascades. First, an E2 transiently binds E1 for generation of a thioester-linked E2~UBL intermediate, which then interacts with an E3. For RING E3s, the UBL is transferred from E2 to an E3-associated target's lysine, producing an isopeptide-bonded target~UBL complex. E2 core domains are sufficient for binding E1s and RING E3s (*11*). Contacts beyond E2 cores often mediate pathway-specific interactions. A unique N-terminal extension on Nedd8's E2, Ubc12, binds both E1 and E3 (*12*–*16*). Nedd8 transfer from Ubc12 to cullins involves a "dual E3" mechanism (*16*): A RING E3, Rbx1, is essential for cullin neddylation; a co-E3, Dcn1, contains a "potentiating neddylation" domain ($Dcn1^{P}$)

[1]Structural Biology Department, St. Jude Children's Research Hospital, Memphis, TN 38105, USA. [2]Howard Hughes Medical Institute, St. Jude Children's Research Hospital, Memphis, TN 38105, USA. [3]Cell Biology Department, Harvard Medical School, Boston, MA 02115, USA.

*Present address: Division of Biological Sciences, University of California–San Diego, La Jolla, CA 92093, USA.
†To whom correspondence should be addressed. E-mail: brenda.schulman@stjude.org